BNL-211962-2019-TECH
CBETA/043

ERL Timing and optimized CBETA models

R. Koscica, S. Peggs

May 2019

Collider Accelerator Department
Brookhaven National Laboratory

U.S. Department of Energy
USDOE Office of Science (SC), Nuclear Physics (NP) (SC-26)

DISCLAIMER

ERL Timing and Optimized CBETA Models

Internal Report CBETA-43

ERL Group, Professor Hoffstaetter

Rosalyn Koscica

May 2019

Contents

1 Introduction

This project develops a method of finding instrument settings that minimize the power load on accelerating radio-frequency (RF) cavities in an energy recovery linac (ERL). A general symmetry theory, which has been developed in detail [1] and was previously tested in simple ERL models, will be used to optimize more detailed models of the Cornell Brookhaven ERL Test Accelerator (CBETA). CBETA specifications are detailed in Fig. 1.

Due to the high overlap with previous work, this report briefly summarizes the relevant outcomes of older ERL symmetry models; however, the reader is encouraged to consult [1] for a more comprehensive coverage of these topics. This report will focus primarily on extensions of symmetry modeling toward more complex systems, including multi-particle beams or CBETA-specific cavity tracking.

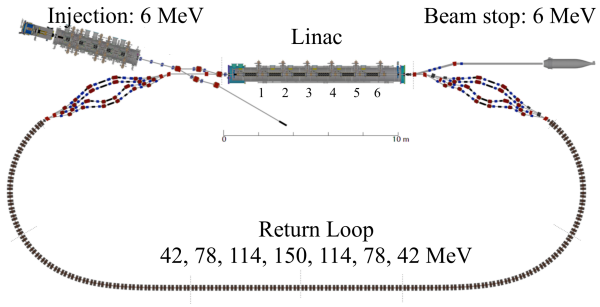

Figure 1: CBETA layout [2]. CBETA has 4 physically distinct return loops and a linac that holds 6 evenly spaced RF cavities. A 6 MeV injected electron beam accelerates to 150 MeV over 4 linac passes, and the beam returns to 6 MeV after 4 more decelerating passes. The 150 MeV beam is intended for use in experiments.

1.1 Optimization System

Consider a $\frac{M}{2}$-turn ERL with N cavities and M linac passes. Individual passes and cavities use indices m and n, such that $1 \leq m \leq M$ and $1 \leq n \leq N$. The m^{th} return loop is between the m^{th} and $(m+1)^{th}$ linac passes.

In an ERL without shared return loops, the degrees of freedom include: $(M-1)$ independent loop lengths, N cavity phases, and N cavity voltages. The objectives include minimization of N cavity loads, where load is defined as the net beam energy gain within a single cavity over the full ERL run. In addition, $(M-1)$ beam energies during return loops must meet design targets to ensure proper beam control.

There are a total of $(2N + M - 1)$ degrees of freedom, which can be varied to satisfy $(N + M - 1)$ objectives. In CBETA, there are only $\frac{M}{2} = 4$ shared return loops; this gives 16 degrees of freedom and 13 objectives.

ERL symmetry can reduce the size of the optimization system. Symmetry exists when the decelerating beam encounters an exactly reversed sequence of energy steps and electric field profiles as it initially experienced during acceleration. To create symmetry, we make the phase and voltage settings of the $(N-n+1)^{th}$ cavity dependent on those of the n^{th} cavity. Degrees of freedom are then: $\frac{M}{2}$ independent loop lengths, $\frac{N}{2}$ phases, and $\frac{N}{2}$ voltages.

A symmetric ERL has only $[\frac{N}{2}]$ independent loads, where the Gauss bracket denotes the floor of a number. The m^{th} and $(M-m)^{th}$ returning beams have identical energy: only $\frac{M}{2}$ loop energy objectives are required. If return loops with index $m < \frac{M}{2}$ can be calibrated post-optimization to match the beam energy, then these loops need not be considered as target energy objectives. Then, the system needs only considers the design target of the highest energy beam, which must be met if the beam is to be used in experiments.

If the objectives only consider the maximum beam energy, the symmetric ERL has a total of $N + \frac{M}{2}$ degrees of freedom, which must satisfy $[\frac{N}{2}] + 1$ objectives. If an optimization system with equal numbers of variables and constraints is desired, one can set all $\frac{N}{2}$ voltages and the first $(\frac{M}{2} - 1)$ loop lengths to reasonable constant values. In CBETA, symmetry yields 10 possible degrees of freedom and 4 objectives.

1.2 Symmetry Theory

Our goal is to create a decelerating sequence of beam energy and electric field encounters that is identical, but reversed in order, to the accelerating sequence. In an ERL, symmetry in the cavity fields can exist if the geometry of the n^{th} cavity is the mirror image of that of the $(N-n+1)^{th}$ one, with respect to the center of the linac.

Before examining a full ERL, consider two cavities (A and B) arranged end-to-end, in a mirror symmetric way about a central point. In the later cavity, B, the beam should decelerate to its original energy over an identical transit time as the acceleration in A took: $T_B = T_A$. The RF phase of cavity B when the particle enters, $\phi_{\text{in},B}$, must have a specific relation to the cavity A input phase. To find this relation, consider the electric field within A,

$$\mathcal{E}_A(s,t) = \mathcal{E}_{A0}(s)\sin\big(\omega(t - t_{\text{in,A}}) + \phi_{\text{in},A}\big), \tag{1}$$

where ω is the RF frequency, the particle enters cavity A at time $t_{\text{in,A}}$, and $\phi_{\text{in},A}$ is the input phase that can be used as a degree of freedom. The spatial RF field dependence is given by $\mathcal{E}_{A0}(s)$, and by convention it is chosen to start with a positive value in the first cell of a multi-cell cavity. For cavities with an odd number of cells, the spatial dependence is a symmetric function about the center; for an even number of cells, it is an anti-symmetric function. This means that $\mathcal{E}_{B0}(L-s) = \pm\mathcal{E}_{A0}(s)$. The sign (+) is for odd and (−) is for even numbers of cells per cavity.

For symmetry in A and B, the electric field at distance s from the start of A must be opposite the field at distance s from the end of B. Suppose each cavity has length L_s, and the linac has total length $L \geq 2L_s$,

$$\mathcal{E}(L_s - s) = -\mathcal{E}(s) \tag{2a}$$

$$\mathcal{E}_B(L - s, t(L_s - s)) = -\mathcal{E}_A(s, t(s)) \tag{2b}$$

$$\begin{aligned}\mathcal{E}_B(L - s, t(L_s - s)) \\ = \pm\,\mathcal{E}_{A0}(s)\sin(\omega(T_A - t(s) + t_{\text{in,A}}) + \phi_{\text{in},B}) \\ = -\,\mathcal{E}_{A0}(s)\sin(\omega(t(s) - t_{\text{in,A}}) + \phi_{\text{in},A}).\end{aligned} \tag{2c}$$

Solving for the unknown cavity B input phase, $\phi_{\text{in},B}$, we find conditions for cavities with an odd or even number of cells,

$$\begin{aligned}\phi_{\text{in},B} &= -\phi_{\text{in},A} - \omega T_A = -\phi_{\text{out},A} \qquad \text{[odd]} \\ \phi_{\text{in},B} &= \pi - \phi_{\text{in},A} - \omega T_A = \pi - \phi_{\text{out},A}. \quad \text{[even]}\end{aligned} \tag{3}$$

If $\phi_{\text{in},B}$ fulfills this phase condition, for any arbitrary choice of $\phi_{\text{in},A}$, then the deceleration in B will exactly reverse the acceleration from A. We now extend the 2-cavity argument to find phase conditions for a full multi-turn ERL.

In an N-cavity, M-pass ERL, the beam encounters each of N cavities during a single pass, for M total encounters per cavity. The input phase, ϕ_{in}, is not as useful a measure as in the 2-cavity case. Instead, let $\phi_{0,n}$ be the RF phase of cavity n at beam injection time $t = 0$,

$$\begin{aligned}\phi_{0,n} &= \phi_{\text{in},mn} - \omega t_{\text{in},mn} \\ &= \phi_{\text{out},mn} - \omega t_{\text{out},mn},\end{aligned} \tag{4}$$

where the mn subscript indicates the m^{th} pass of cavity n. In the 2-cavity example, A and B represented a symmetric acceleration-deceleration pair. In the full ERL, the m^{th} encounter of cavity n is the mirror symmetric pair of the $m' = (M - m + 1)^{th}$ encounter of cavity $n' = (N - n + 1)$, where the primed encounter occurs first, *i.e.* $m > m'$. If N is odd, then the central cavity will act as its own pair, but the phase condition will follow the same form as the other pairs. Our goal here is to find the initial phase of cavity n in terms of the known $\phi_{0,n'}$. Inserting these pair designations into the phase conditions from Eq. (3),

$$\begin{aligned}\phi_{0,n} &= -\phi_{0,n'} - \omega t_{\text{total}} \qquad \text{[odd]} \\ \phi_{0,n} &= \pi - \phi_{0,n'} - \omega t_{\text{total}}, \quad \text{[even]}\end{aligned} \tag{5}$$

where the beam travels through the full ERL, from injector to beam stop, over a total time interval, $t_{\text{total}} = \omega t_{\text{in},mn} + \omega t_{\text{out},m'n'}$. This is more generally stated as

$$\boxed{\phi_{0,n} = a - \phi_{0,n'} - \omega t_{\text{total}},} \tag{6}$$

where a indicates some constant offset based on the time and spatial dependence of the system, as seen in Table 1.

For t_{total} to accurately describe the total transit time over the ERL, the time of flight of the return loop between acceleration and deceleration must be set,

$$\boxed{t_{\text{loop},\frac{M}{2}} = t_{\text{total}} - 2t_{\text{out},\frac{M}{2}N},} \tag{7}$$

where $t_{\text{out},\frac{M}{2}N}$ is the time from beam injection to the end of the last accelerating pass. Time t_{total} then becomes a degree of freedom.

The Eq. (6) and Eq. (7) conditions are sufficient to guarantee that every stage of beam acceleration is matched by an equivalent deceleration. At beam stop, the beam will have the same energy as at injection. Symmetry guarantees that each pair of cavities will have a net load of zero; however, an individual cavity could still have nonzero load if its pair has an equal, opposite load. Optimization is still needed to minimize the power load on each individual cavity.

a	$\sin(\omega\Delta t)$	$\cos(\omega\Delta t)$
s Symmetric	0	π
s Anti-symmetric	π	0

Table 1: Phase conditions: the value of a in Eq. (6) for ideal symmetric/anti-symmetric spatial (s) dependence, and for ideal sin/cos time (t) dependence when when $\phi_{\text{in}} = 0$. If the spatial field is neither symmetric (odd cells) nor antisymmetric (even cells), or if the time dependence is neither $\sin(\omega\Delta t)$ nor $\cos(\omega\Delta t)$ when $\phi_{\text{in}} = 0$, then a may not be as easily determined.

1.3 Relevant Previous Models: TL, UR, FT

To test ERL symmetry optimization, models of CBETA beam flight were constructed in Mathematica. Models consider a transversely on-axis particle that encounters only drift pipes or cavities. The beam traverses a cavity in time T_{mn}, where its energy changes by some ΔE_{mn}. If a modeled cavity is shorter than the physical length in CBETA, the model element is centered within the space, and drifts on either side are extended to compensate for the missing length. CBETA cavities have an elliptical geometry with 7 cells [2].

In the thin lens (TL) model, cavities have zero length and deliver a delta-function acceleration. If voltage is designated V and particle charge q, the cavity models time and energy as,

$$\Delta E_{\text{TL}} = qV\cos(\phi_{\text{in}}), \qquad T_{\text{TL}} = 0. \tag{8}$$

The ultra-relativistic (UR) model treats the beam as having speed $v = c$ within a 7-cell cavity of length corresponding to 7 stacked pillboxes,

$$\Delta E_{\text{UR}} = qV\cos(\phi_{\text{in}}), \qquad T_{\text{UR}} = \frac{L}{c} = \frac{7\pi}{\omega}. \tag{9}$$

The finite time-tracked (FT) model accounts for non-ultrarelativistic particle speeds by starting with an averaged cavity transit time, T_{FT}. From T_{FT}, we find velocity v, which is used to calculate the total change in momentum P_{FT} and energy change E_{FT}, in a set of coupled equations. The FT model approximates the effect of a single accelerating pillbox cavity,

$$T_{\text{FT}} = \frac{L}{2}\left(\frac{1}{v_{\text{in}}} + \frac{1}{v_{\text{out}}}\right), \qquad \Delta P_{\text{FT}} = \frac{q}{\omega}E_{\text{in}}[\cos(\omega T_{\text{FT}} + \phi_{\text{in}}) - \cos(\phi_{\text{in}})]. \tag{10}$$

Models with CBETA specifications and these three cavity types have been previously constructed with a single, transversely on-axis particle. These were optimized using Newton's method to reduce cavity load and achieve the CBETA peak energy target of 150 MeV. The optimized solutions yield objective output values within 100 μeV precision of targets [1].

2 Longitudinal Beam Tilting

Since the single-particle ERL has been successfully optimized in the simple TL, UR, and FT models, we next consider a beam where particles differ only in longitudinal position and energy. If particles are offset from the optimized path, then the beam final energy may differ from that of the optimized case. This may result in particle containment problems if the energy spread of the beam is too large at beam stop.

Using relative phase space coordinates, $(x, p_x, y, p_y, z, \delta)$, the optimized single-particle path is defined at coordinates $(0, 0, 0, 0, 0, 0)$, and all other particles in this beam occur at some $(0, 0, 0, 0, z, \delta)$. For brevity, particle coordinates will be written as (z, δ), where $\delta = \frac{E_z - E_{z0}}{E_{z0}}$ is a normalized quantity. If a beam with a Gaussian distribution of (z, δ) particles is sent through an FT model ERL, the output distribution is visually tilted from the input (Fig. 2, left). By controlling the distribution of input particles, the energy spread at ERL input and output can be made equal (Fig. 2, middle), or the energy spread at beam stop can be minimized for optimal collection of output particles (Fig. 2, right).

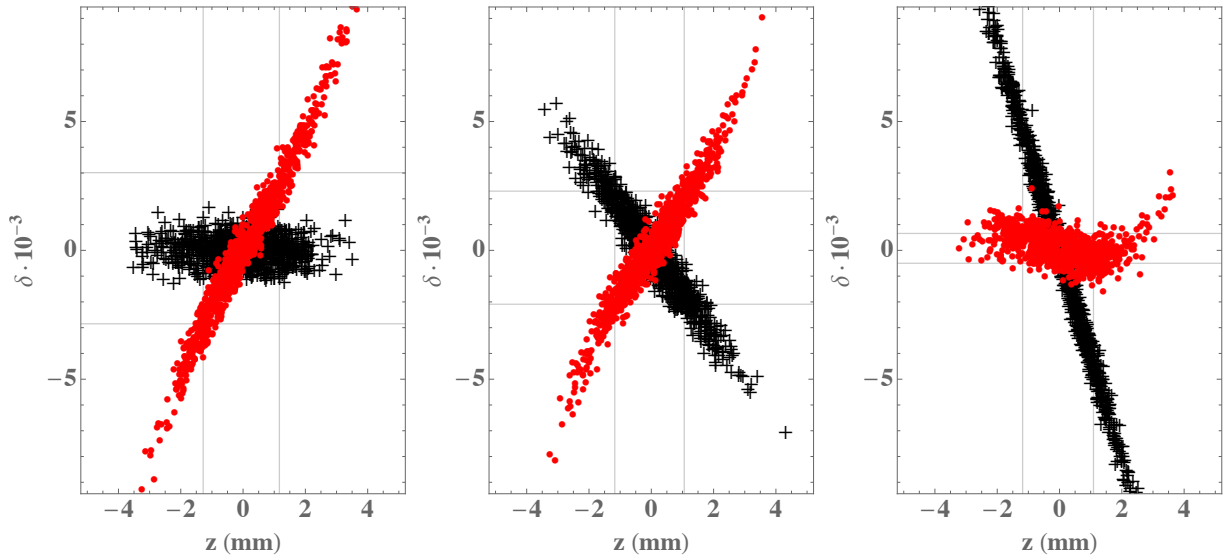

Figure 2: Injected (+) and final (•) particle distributions of the FT model ERL in longitudinal (z, δ) phase space. Left: Gaussian input with standard deviations of $\sigma_z = 1.1$ mm, $\sigma_\delta = 5 \cdot 10^{-4}$ results in highly tilted output. Middle: matrix-tilted input results in equal, opposite output tilt. Right: highly tilted input results in minimized output δ spread. Vertical and horizontal lines indicate one standard deviation of output distribution z and δ.

2.1 Symmetric Beam Tilt Derivation

The energy spread, σ_δ, of the beam at injection and beam stop can be made equal if the initial distribution is formed with a particular tilt in longitudinal phase space. This tilt is found by comparing transfer matrices of one offset particle over both forward and backward ERLs. The forward matrix M transforms injection phase space coordinates to those at beam stop,

$$\begin{bmatrix} z_{\text{stop}} \\ \delta_{\text{stop}} \end{bmatrix} = \begin{bmatrix} M_{11} & M_{12} \\ M_{21} & M_{22} \end{bmatrix} \begin{bmatrix} z_{\text{inj}} \\ \delta_{\text{inj}} \end{bmatrix}. \tag{11}$$

Similarly, the reverse matrix R models a particle that entered at beam stop, traveled backward through all ERL paths, and exited at injection,

$$\begin{bmatrix} -z_{\text{inj}} \\ \delta_{\text{inj}} \end{bmatrix} = \begin{bmatrix} R_{11} & R_{12} \\ R_{21} & R_{22} \end{bmatrix} \begin{bmatrix} -z_{\text{stop}} \\ \delta_{\text{stop}} \end{bmatrix}. \tag{12}$$

By equating like terms in Eq. (11 and an inverted Eq. 12), we find $M_{11} = M_{22}$ in the matrices. Since the goal is to achieve identical initial and final energy spread, the M matrix must preserve the magnitude of the δ component at some z. The transfer matrix can be written with a linear coordinate relation, $\delta = Az$, for small initial offsets of the two general phase space coordinates,

$$\begin{bmatrix} z \\ -Az \end{bmatrix} = \begin{bmatrix} M_{11} & M_{12} \\ M_{21} & M_{11} \end{bmatrix} \begin{bmatrix} z \\ Az \end{bmatrix}. \tag{13}$$

Resolving the matrix equation into two linear equations then yields the scale factor between z and δ,

$$A = \frac{1 - M_{11}}{M_{12}} = -\frac{M_{21}}{1 + M_{11}}. \tag{14}$$

If A is used as the slope of the tilted input beam, the ERL input and output distributions have mirrored slopes and arrangements relative to the optimized particle path (Fig. 2, middle).

2.2 Model Construction

Beam effects are tested on the TL, UR, and FT models, which have been modified slightly from their original state to report the results of particles offset from the optimized one. A beam is generated with a Gaussian distribution of approximately realistic proportions: standard deviations are $\sigma_z = 1.1$ mm and $\sigma_\delta = 5 \cdot 10^{-4}$. In Fig. 2, the leftmost plot indicates the inputs and outputs of an untilted beam.

To create a tilted beam (Fig. 2, middle), the ERL transfer matrix is formed by injecting a single test particle with small z or δ offset on the order of 10^{-7} m or 10^{-7}, respectively, and measuring the output. From Eq. (13), the matrix elements are,

$$\begin{bmatrix} M_{11} & M_{12} \\ M_{21} & M_{11} \end{bmatrix} = \begin{bmatrix} \frac{z_{\text{stop}}}{z_{\text{inj}}}(\delta_{\text{inj}} = 0) & \frac{z_{\text{stop}}}{\delta_{\text{inj}}}(z_{\text{inj}} = 0) \\ \frac{\delta_{\text{stop}}}{z_{\text{inj}}}(\delta_{\text{inj}} = 0) & \frac{z_{\text{stop}}}{z_{\text{inj}}}(\delta_{\text{inj}} = 0) \end{bmatrix}. \tag{15}$$

The A parameter from Eq. (14) is the slope needed for symmetric tilt. In longitudinal phase space, a line with this slope is generated and superimposed on all beam coordinates. Slight non-linearity may occur in the output beam if the (z, δ) injection coordinates exceed the linear regime of the matrix calculation. However, this can be compensated for by calculating a matrix using test particles of larger offset.

Symmetric	UR	FT
Slope A	-0.6714	-1.7748
Inj. Angle (°)	-33.8772	-60.6006
Pass 4 Angle (°)	-0.0042	-1.0045
Stop Angle (°)	41.2810	63.4172
$\sigma_{E,\text{inj}}$ (keV)	5.3765	12.0839
$\sigma_{E,\text{stop}}$ (keV)	6.6398	13.5756
$\sigma_{\delta,\text{stop}}/\sigma_{\delta,\text{inj}}$	1.2350	1.1234

Table 2: Optimal beam tilt parameters for a symmetric injector-stop energy spread, found for a typical-sized CBETA beam ($z =$ 1.1 mm, $\delta = 5 \cdot 10^{-4}$) with matrices. "Angle" describes the counter-clockwise angle between the positive z-axis in longitudinal phase space and a linear fit of the beam. The beam of order 10^{-3} in both coordinates is much larger than the $z = 10^{-7}$ m,$\delta = 10^{-7}$ offset used to calculate the matrix, resulting in some nonlinear curvature in the output beam.

For a beam with the energy spread minimized at the end of the ERL (Fig. 2, right), the appropriate tilt of the injected distribution is determined by scanning over the possibilities. The slope of the line superimposed over the Gaussian distribution is modified in uniform intervals until the σ_δ at beam stop has reached a minimum value. Again, non-linear distortions to the shape of the output beam may arise if the input beam is larger than the linear regime of the matrix.

3 ERL Symmetry: Bmad Simulator

The effectiveness of the Mathematica-based TL, UR, and FT models is limited by the accuracy of the equations used to model the RF cavity as a time and energy coordinate transform. Mathematica models are advantageous due to their rapid simulation speed, but they do not describe the CBETA behavior completely. To model the behavior of the ERL in a more realistic manner, the time and energy interactions between a cavity and beam must account for RF fields directly. This is accomplished using the Bmad simulator, which can track particle time and energy through cavities using Runge Kutta integration.

In a Bmad hybrid lattice, like in the Mathematica models, the CBETA system is modeled as a series of alternating drifts and cavities. Drifts are represented by identity transfer matrices that increase the time of the system, but do not otherwise alter particle coordinates. The hybrid lattice does not consider transverse effects of non-accelerating components, such as return loop optics; all such elements are replaced by drift pipes in the hybrid model. The cavities use Runge Kutta integration with either fixed or variable step size (`fixed step time runge kutta` or `time runge kutta`, in the Bmad language [3]). The RF fields can be generated by assuming a standard pillbox waveguide (`bmad standard` field option) or interpolating a grid-shaped map of field magnitudes (`fieldmap` option). Use of fieldmap cavities results in slower simulation

speed than the pillbox fields, since fieldmaps have more complex spatial dependencies; they are typically generated in a different program, such as Microwave Studio, to account for the exact geometry of the CBETA cavities.

In our models, Bmad is run via the Tao simulation interface. The Appendix contains the Bmad code required to create an example CBETA hybrid lattice with pillbox cavities and enforce ERL symmetry, as well as the Tao script required to properly activate the Bmad code. With slight modifications to the cavity and overlay element code, the Bmad hybrid lattice can be adapted to use fieldmap cavities instead.

To measure the tolerance of optimization objectives to errors in machine settings, each input can be varied by a slight, known amount to measure the reaction of the objectives. Combining these slopes via error propagation equations will result in values for system error tolerance when multiple inputs are simultaneously fluctuating. Error sensitivity and tolerance are further explored in the original ERL symmetry report [1].

Objective (eV)	Pillbox (Bmad)	Fieldmap (Bmad)
$\Delta E_{\text{loop},4}$	$8.5149{\cdot}10^{-1}$	$-7.2021{\cdot}10^{-1}$
$E_{\text{load},1}$	$-2.6786{\cdot}10^{-4}$	-4.6014
$E_{\text{load},2}$	$-3.1140{\cdot}10^{-5}$	-2.1626
$E_{\text{load},3}$	$-8.4966{\cdot}10^{-5}$	7.5983
$E_{\text{load},4}$	$6.4570{\cdot}10^{-2}$	7.5821
$E_{\text{load},5}$	$6.7490{\cdot}10^{-2}$	-2.1718
$E_{\text{load},6}$	$7.6797{\cdot}10^{-2}$	-4.5920
Energy (MeV)	-	-
$E_{\text{loop},1}$	42.1801	42.0116
$E_{\text{loop},2}$	78.2023	78.0316
$E_{\text{loop},3}$	114.226	114.125
$E_{\text{loop},4}$	150.000	150.000
$E_{\text{loop},5}$	114.226	114.125
$E_{\text{loop},6}$	78.2023	78.0316
$E_{\text{loop},7}$	42.1801	42.0116
$E_{\text{loop},8}$	6.00000	6.00000
Input	-	-
$\phi_{0,1}$ (°)	0.3851	4.0930
$\phi_{0,2}$ (°)	-41.5841	27.3243
$\phi_{0,3}$ (°)	-83.5456	47.4272
t_{total} (μs)	2.15429	2.15467
$t_{\text{loop},1}$ (μs)	0.26456	0.23729
$t_{\text{loop},2}$ (μs)	0.26455	0.23807
$t_{\text{loop},3}$ (μs)	0.26456	0.23731
qV_n (MeV)	6.0500	6.0500

Table 3: Optimized objectives, beam energies, and input setting solutions (phase, total time, loop time of flights, and cavity voltage) after numerical optimization of ϕ_0 and t_{total} in Bmad CBETA hybrids.

3.1 Hybrid with 7-Cell Pillbox Cavities

By default, Bmad approximates cavities as series of stacked pillbox waveguides. When Bmad `lcavity` element attributes are set in the `bmad standard field calculation` with the multi-cell `longitudinal mode 0` option, the transversely on-axis electric field follows the spatial dependence,

$$\mathcal{E}(s) = 2G\sin(ks)\sin(\omega t + \phi_{\text{in}}), \qquad (16)$$

where G is the accelerating gradient of a $v = c$ particle traveling through the cavity. This *pseudo* TM_{010} field resembles a 1^{st} harmonic pillbox, except that the field is shifted in space to give the correct 0^{th} harmonic symmetry [3]. This results in a field that better models the field produced by elliptical cavities than a true 0^{th} harmonic pillbox.

Tracking particles through pillbox cavities with fixed or variable step Runge Kutta results in energy differences of less than 1 meV. The hybrid model uses variable step Runge Kutta beam tracking (Bmad `time runge kutta` option), and it is optimized using the Levenberg-Marquardt differential algorithm. Optimized values are given in Table 3. Note that all values of the form ωt are 2π periodic; for instance, t_{total} may be increased or decreased by any offset of $\frac{2\pi}{\omega}$ without affecting the solutions.

3.2 Hybrid with CBETA Fieldmap Cavities

Since CBETA cavities have an elliptical geometry [2], the Bmad pillbox fields are not the best model. A more accurate model, albeit more computationally intensive, uses fieldmaps: grids of electric and magnetic field magnitudes throughout the space of the cavity. Fieldmaps account better for the geometric effects of the physical cavity. A transversely on-axis particle will only experience a field in the longitudinal direction (Fig. 3).

The CBETA fieldmap visually appears to be symmetric about the cavity center. However, if the list of on-axis field intensities (from $s = 0$ to $s = L$) is subtracted from a reversed list (from $s = L$ to $s = 0$), there is a maximum of 1.32% discrepancy between the forward and backward field sequences. Evidently, this discrepancy is significant: if two fieldmap cavities are arranged in linear sequence (bringing one electron from 6 MeV to 12 MeV, and back to 6 MeV), as in the 2-cavity symmetry condition derivation, symmetry conditions lead to particle acceleration and deceleration that differ by energies on the order of 1-10 keV. With such energy asymmetry present in a simple 2-cavity scenario, adding more cavities is most likely to result in increasing asymmetry, and creating a symmetric ERL quickly becomes unfeasible.

If the fieldmap asymmetry is problematic, then one may expect resolution when using a symmetric fieldmap. Tests of custom-generated ideal sinusoidal fieldmaps, which have perfect symmetry by mathematical definition, do appear to indicate that this is a reasonable assumption. A modified CBETA fieldmap is constructed by averaging the original and reversed lists of field points. This way, the grid points that had resulted in a 1.32% discrepancy have been shifted to midway between the asymmetric magnitudes, and the fieldmap is now symmetric. When tested in the 2-cavity scenario, the symmetry conditions give acceleration and deceleration that differ by less than 1 eV: a vast improvement over the original, un-averaged fieldmap. Using this modified map, we then return to the hybrid ERL.

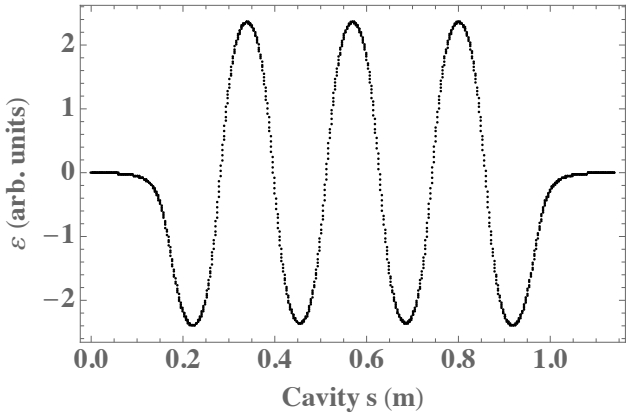

Figure 3: Spatial dependence of the CBETA fieldmap along the central axis of the cavity.

The Bmad hybrid lattice operates similarly with a pillbox or fieldmap cavity. However, while pillbox cavities follow a $\sin(\omega\Delta t + \phi_{\text{in}})$ time dependence, fieldmaps are varied as $\cos(\omega\Delta t + \phi_{\text{in}})$. Hence, following Table 1, the phase condition on fieldmap cavities must include an extra π to compensate for the different time dependence. A similar optimization scheme is used, resulting in solutions of 1-10 eV precision (Table 6). The larger magnitude of post-optimization objective values (1-10 eV, as opposed to under 1 eV) may indicate higher calculation noise when fieldmap cavities are used.

Another potential solution to the fieldmap asymmetry, though unexplored in this study, is to use original and reversed fieldmaps in a symmetric arrangement. That is, the original fieldmap will remain unmodified, while a second map will be created using an exactly reversed s dependence. Since CBETA has an even number of cavities, with $N = 6$, we can make the linac symmetric by putting forward-facing fieldmaps in the first 3 cavities and backward-facing maps in the latter 3. Hence, during acceleration and deceleration, the particle should encounter similar fields despite the lack of symmetry in an individual cavity. This potential solution has not been tested in Bmad.

4 Conclusions

In this project, ERL symmetry has been successfully implemented in simplified CBETA simulations of transversely on-axis particles traveling through drift and cavity elements. In cases where the RF fields are symmetric within the cavities, the phase conditions derived in Eq. (6) and Eq. (7) successfully establish symmetry. Following this arrangement, the tested systems have been optimized using the symmetry-reduced variable-constraint system to minimize the load and achieve the target peak beam energy.

In the cases considered, only the load and maximum beam energy have been used as optimization goals. Future CBETA simulations may expand this optimization system to consider additional parameters, such as intermediate beam energy or beam energy spread. Detailed properties of non-accelerating elements, *e.g.* loop optics and bending magnets, should also be considered in simulation before attempting to apply ERL symmetry to a physical system; transverse effects may lead to more complex symmetry requirements than identified in the purely longitudinal models considered here.

5 Acknowledgements

I acknowledge Professor Hoffstaetter for conceptual work with the ERL symmetry; Dr. David Sagan and William Lou for assistance with the Bmad and Tao simulators; Nilanjan Banerjee for contributions to the FT model and general theory; and Gayathrini Premawardhana for assistance with the Mathematica beam modeling.

References

[1] R. Koscica, N. Banerjee, G. H. Hoffstaetter, W. Lou, G. Premawardhana, "Energy and RF Cavity Phase Symmetry Enforcement in Multi-turn ERL Models," Apr. 2019, arXiv:1904.04332

[2] G. H. Hoffstaetter, D. Trbojevic, C. Mayes, N. Banerjee, J. Barley, I. Bazarov, *et al.*, "CBETA Design Report, Cornell-BNL ERL Test Accelerator," Jun. 2017, arXiv:1706.04245

[3] D. Sagan, *The BMAD Reference Manual*, Dec. 2017, https://www.classe.cornell.edu/bmad/manual.html

6 Appendix

6.1 Mathematica CBETA Model

The Mathematica TL, UR, and FT models use the following basic framework to model a single on-axis electron in a symmetric ERL with $N = 6$ cavities and $M = 8$ linac passes. A modified version of this code is used in cases where symmetry may be broken, *e.g.* with particles of (z, δ) offset or when measuring the sensitivity to ERL setting error.

```
erlsim[phiin_, wtTot_] := Module[{
   phi = Flatten[{phiin, Pi - wtTot - Reverse[phiin]}],
   wtime = 0, energy = E0, eold = E0, load = {0, 0, 0, 0, 0, 0}, ePeak = 0
  }, Do[Do[
    (* CAVITY *)
    {wtime, energy} = cavity[wtime, energy, phi[[n]]];
        load[[n]] = load[[n]] + (energy - eold); eold = energy;
        If[m == 4 && n == 6, ePeak = energy - 150 000 000];
    (* DRIFT *)
    If[n < 6, wtime = wtime + w * ldrift / v[energy]];
    , {n, 6}];

   (* RETURN LOOP *)
   If[m < 4, wtime = wtime + wtloop[[m]],
    If[m == 4, wtime = wtime + (wtTot - 2 wtime),
     If[m < 8, wtime = wtime + wtloop[[8 - m]]]]];
   , {m, 8}];
  Flatten[{ePeak, load}]]
```

This particular code is from the TL model: hence the presence of `Pi` in the phase condition from Eq. (6) on line 2. The `cavity[]` module maps input time, energy, and ϕ_{in} phase into output time and energy values, and can take the form of a TL, UR, or FT equation system. `E0` is the particle energy at injection in eV, `w` is the RF angular frequency in rad/s, `ldrift` is the length between the end of a cavity and the beginning of the subsequent cavity, and `v[energy]` is the particle velocity. Time is scaled by a factor of `w` and measured in radians for convenience. ERL input parameters include `phiin`, an array of input phases for the first 3 cavities; `wtTot`, the scaled version of t_{total} from Eq. (7); and `wtloop`, an array of 3 times of flight for the first 3 return loops, which are reversed but identical for the last 3 loops in a symmetric system. This code creates symmetry on the order of 10^{-7} eV. The outputs, peak energy offset `ePeak` and the array of cavity `load` values, are then optimized with Newton's method toward the target value 0.

6.2 Bmad CBETA Hybrid Model

The following Bmad code generates a sample CBETA hybrid lattice with only drift pipes and 7-cell pillbox cavities. Numbers are consistent with the optimized solution only if the solution values in Table 3 take precedence; this is indicated by the `call, filename` command, which invokes the optimized solution as

an external list of attribute input values. Numbers unstated in the table are already optimized, and thus remain unchanged, in this code. Due to CBETA convention, the first cavity after the injector is designated `RD1CAV06` and the last `RD1CAV01`. More information on Bmad code formatting can be found in the Bmad manual [3].

```
parameter[lattice]      = "CBETA hybrid 6c8p lattice"
parameter[geometry] = Open
parameter[e_tot]    = 6e6
parameter[particle]                 = Electron
parameter[absolute_time_tracking]     = T
beginning[x_position]      = 12.971553
beginning[z_position]      = 11.5139582
beginning[theta_position] = -0.26179938779915
beginning[s]         = 8.53583
beginning[beta_a]    = 0.34295156880491
beginning[alpha_a]   = 0.72321443195869
beginning[beta_b]    = 1.0004383576185
beginning[alpha_b]   = 0.1884214500459

! ===== CAVITIES =====
RD1CAV: Lcavity, descrip = "3DMODEL=7103-210_STL/7103-210_bare.blend",
  L = 0.807133540769230717338,
   RF_FREQUENCY = 1.3E9, , PHI0 = 0,
   N_CELL = 7, N_REF_PASS = 1, DS_STEP = 0.01,
   tracking_method = time_runge_kutta, mat6_calc_method = tracking,
   AUTOSCALE_AMPLITUDE = F, AUTOSCALE_PHASE = F,  LONGITUDINAL_MODE = 0
RD1CAV01: RD1CAV
RD1CAV02: RD1CAV
RD1CAV03: RD1CAV
RD1CAV04: RD1CAV
RD1CAV05: RD1CAV
RD1CAV06: RD1CAV

!===== INTERCAVITY DRIFTS =====
PIPEA: Pipe, L = 0.6033278592307693, DS_STEP = 0.01, aperture = 10
PIPEB: Pipe, L = 0.6033278592307693, DS_STEP = 0.01, aperture = 10
PIPEC: Pipe, L = 0.6033278592307693, DS_STEP = 0.01, aperture = 10
PIPED: Pipe, L = 0.6033278592307693, DS_STEP = 0.01, aperture = 10
PIPEE: Pipe, L = 0.6033278592307693, DS_STEP = 0.01, aperture = 10

!===== RETURN LOOPS =====
LOOP1: Hybrid, type = "NBPIPE",
   DELTA_REF_TIME = 2.368749995073098E-07,
   mat6_calc_method = Taylor, tracking_method = Taylor,
   {1: 1|1},
   {2: 1|2},
   {3: 1|3},
   {4: 1|4},
   {5: 1|5},
   {6: 1|6}
LOOP2: Hybrid, type = "NBPIPE",
   DELTA_REF_TIME = 2.368468384497991E-07,
   mat6_calc_method = Taylor, tracking_method = Taylor,
   {1: 1|1},
   {2: 1|2},
```

```
    {3: 1|3},
    {4: 1|4},
    {5: 1|5},
    {6: 1|6}
LOOP3: Hybrid, type = "NBPIPE",
    DELTA_REF_TIME = 2.368368820576889E-07,
    mat6_calc_method = Taylor, tracking_method = Taylor,
    {1: 1|1},
    {2: 1|2},
    {3: 1|3},
    {4: 1|4},
    {5: 1|5},
    {6: 1|6}
LOOPP: Hybrid, type = "NBPIPE", !L =71.2846659779234,
    DELTA_REF_TIME = 1.190803262451950E-7,
    mat6_calc_method = Taylor, tracking_method = Taylor,
    {1: 1|1},
    {2: 1|2},
    {3: 1|3},
    {4: 1|4},
    {5: 1|5},
    {6: 1|6}
LOOP5: loop3
LOOP6: loop2
LOOP7: loop1

multi_line_la: line[multipass] = (RD1CAV06,PIPEA,
        RD1CAV05, PIPEB,
        RD1CAV04, PIPEC,
        RD1CAV03, PIPED,
        RD1CAV02, PIPEE,
        RD1CAV01)
lat: line = (multi_line_la, LOOP1,
        multi_line_la, LOOP2,
        multi_line_la, LOOP3,
        multi_line_la, LOOPP,
        multi_line_la, LOOP5,
        multi_line_la, LOOP6,
        multi_line_la, LOOP7,
        multi_line_la)
use, lat
 call, filename="../timesymmetry/var1-20190329-nov-p0.in"
```

For fieldmap cavities, the `CAVITY` element in the lattice file is modified to call an external grid file, defined in the `grid field` attribute:

```
CAVITY: Lcavity,
  L = 1.14, n_cell=7, field_calc = fieldmap,
  RF_FREQUENCY = 1.3E9, PHI0 = 0, VOLTAGE = 6.05e6,
  AUTOSCALE_AMPLITUDE = F, AUTOSCALE_PHASE = F,
  FIELD_AUTOSCALE = 1.000060260211661056217735 7,
  grid_field = call::../fieldmaps/MLC-grid-cyl_201904-axisymr.bmad,
  tracking_method = fixed_step_time_runge_kutta, num_steps=1140,
  mat6_calc_method = tracking
```

6.2.1 Lattice Overlay

If a Bmad `overlay` element is added to the hybrid script before the `lat: line` definition, the properties of multiple lattice elements can be controlled at once. The following code imposes the symmetry conditions from Eq. (6) and Eq. (7), as well as ensuring that all cavities have the same RF frequency and gradient. In addition, return loops carrying beams of identical energy are constrained to have the same times of flight. Numbers stated have been found during an intermediate optimization stage. As before, optimized solutions from Table 3 take precedence over the numbers here, particularly for `phi01-3` and `ttot` values.

```
O_LA: overlay = {
    RD1CAV06[phi0]:phi01,
    RD1CAV05[phi0]:phi02,
    RD1CAV04[phi0]:phi03,
    RD1CAV03[phi0]:-freq*ttot -(phi03 -freq*tin03) +freq*tin04,
    RD1CAV02[phi0]:-freq*ttot -(phi02 -freq*tin02) +freq*tin05,
    RD1CAV01[phi0]:-freq*ttot -(phi01 -freq*tin01) +freq*tin06,
    RD1CAV06[RF_FREQUENCY]:freq, RD1CAV06[GRADIENT]:grad1,
    RD1CAV05[RF_FREQUENCY]:freq, RD1CAV05[GRADIENT]:grad2,
    RD1CAV04[RF_FREQUENCY]:freq, RD1CAV04[GRADIENT]:grad3,
    RD1CAV03[RF_FREQUENCY]:freq, RD1CAV03[GRADIENT]:grad3,
    RD1CAV02[RF_FREQUENCY]:freq, RD1CAV02[GRADIENT]:grad2,
    RD1CAV01[RF_FREQUENCY]:freq, RD1CAV01[GRADIENT]:grad1,
    LOOP1[DELTA_REF_TIME]:tloop1,
    LOOP2[DELTA_REF_TIME]:tloop2,
    LOOP3[DELTA_REF_TIME]:tloop3,
    LOOPP[DELTA_REF_TIME]:ttot-2*tacc,
    LOOP5[DELTA_REF_TIME]:tloop3,
    LOOP6[DELTA_REF_TIME]:tloop2,
    LOOP7[DELTA_REF_TIME]:tloop1},
var = {grad1,grad2,grad3,tloop1,tloop2,tloop3,
    freq,ttot,tacc,phi01,phi02,phi03,
    tin01,tin02,tin03,tin04,tin05,tin06},
    freq=1.3E9,
    grad1=7.4956617392384745180 60E+06,
    grad2=7.4956617392384745180 60E+06,
    grad3=7.4956617392384745180 60E+06,
    phi01=-1.0696121575677346345 05E-03,
    phi02=9.4328101956585325843 50E-03,
    phi03=1.2249771440277907458 28E-02,
    ttot=2.1542928294796374831 51E-06,
    tacc=8.9854473012147289253 06E-07,
    tloop1=2.6455540000000018266 95E-07,
    tloop2=2.6455229912000026754 76E-07,
    tloop3=2.6455229912000026754 76E-07,
    tin01=0,
    tin02=4.7114799164803899248 1E-09,
    tin03=9.4186963786385907421 7E-09,
    tin04=1.4124749468169405431 0E-08,
    tin05=1.8830315852594206616 1E-08,
    tin06=2.3535632106787073146 3E-08
```

For fieldmap cavities, the cavity length is different due to fringe fields and the CBETA elliptical geometry. Additionally, since fieldmaps have a $\cos(\omega t)$ spatial dependence, the phase condition is modified according to Table 1. Note that Bmad uses units of rad/2π, instead of rad, to measure phase. The following parameters in the overlay must be altered:

```
RD1CAV03[phi0]: .5 -freq*ttot -(phi03 -freq*tin03) +freq*tin04
RD1CAV02[phi0]: .5 -freq*ttot -(phi02 -freq*tin02) +freq*tin05
RD1CAV01[phi0]: .5 -freq*ttot -(phi01 -freq*tin01) +freq*tin06

grad=5.307017543859649449586868 3E+06,
length=1.14
```

6.2.2 Tao Symmetry Script

Several parameters of the overlay can only be set after a test particle has been tracked through the lattice. For example, `tin05` indicates the particle entrance time to the 5^{th} cavity, yet it is also used in determining the phase of the 5^{th} cavity. These parameters are set based on the data values calculated after Bmad is initialized. Accordingly, the script should be called only after the particle has been tracked through an initial, non-symmetrized lattice. Within the Tao simulation interface, the following script ensures that the tracking-dependent parameters have accurate values:

```
set ele O_LA tin01 = ele::RD1CAV06\1[t] - ele::BEGINNING[t]
set ele O_LA tin02 = ele::PIPEA\1[t] - ele::BEGINNING[t]
set ele O_LA tin03 = ele::PIPEB\1[t] - ele::BEGINNING[t]
set ele O_LA tin04 = ele::PIPEC\1[t] - ele::BEGINNING[t]
set ele O_LA tin05 = ele::PIPED\1[t] - ele::BEGINNING[t]
set ele O_LA tin06 = ele::PIPEE\1[t] - ele::BEGINNING[t]
set ele O_LA tacc = ele::RD1CAV01\4[t] - ele::BEGINNING[t]
```